

Poincaré recurrence and measure of hyperbolic and nonhyperbolic chaotic attractors

Murilo S. Baptista,¹ Suso Kraut,² and Celso Grebogi²

¹*Universität Potsdam, Institut für Physik, Am Neuen Palais 10, D-14469 Potsdam, Germany*

²*Instituto de Física, Universidade de São Paulo, Caixa Postal 66318, 05315-970 São Paulo, Brazil*

(Dated: February 8, 2008)

We study Poincaré recurrence of chaotic attractors for regions of finite size. Contrary to the standard case, where the size of the recurrent regions tends to zero, the measure is not supported anymore solely by unstable periodic orbits inside it, but also by other special recurrent trajectories, located outside that region. The presence of the latter leads to a deviation of the distribution of the Poincaré first return times from a Poissonian. Consequently, by taken into account the contribution of these recurrent trajectories, a corrected estimate of the measure can be provided. This has wide experimental implications, as in the laboratory all returns can exclusively be observed for regions of finite size only.

In dynamical systems one is often interested in calculating asymptotic invariant physical quantities that are independent of the initial conditions and invariant under the evolution of the dynamics. Those invariant quantities are the main subject of ergodic theory, which was suitably applied to chaotic dynamical system, producing important average estimates, like Lyapunov exponents and dimensions [1]. Chaotic systems are ergodic and therefore time averaged quantities calculated from a typical trajectory can also be calculated through space integrals using the natural measure of a chaotic attractor, which is related to the probability of finding a typical trajectory in some region of the attractor. Hence, the calculation of this measure yields essential observable quantities of chaotic systems.

It is well accepted that the support of the measure as well as properties of the attracting set are hierarchically approached by the set of unstable periodic orbits (UPOs) which are embedded in the chaotic attractor [2, 3, 4]. For hyperbolic systems this approach allows a reconstruction of the fractal dimension of a chaotic attractor through UPOs [2, 5]. For the important class of nonhyperbolic chaotic attractors, i. e., when there exist UPOs whose stable and unstable manifolds exhibit tangencies, only numerical results for averages in phase space exist, suggesting that, on average, the nonhyperbolic regions do not play a special role [6].

Recently, an exact result on the probability distribution of the series of first return times (FRTs) $\tau_i, i = 1, \dots, N$ for measurable dynamical systems (including nonhyperbolic ones) was provided [7]. It was proven that the distribution of the FRTs, if the return time is larger than some constant value and the size of the region goes to zero, approaches the Poissonian $\rho(\tau, \mathcal{B}) = \mu \exp^{-\mu\tau}$, with μ being the probability density measure of the region \mathcal{B} of size ϵ , as also discussed in [8, 9]. Thus,

$$\lim_{\epsilon \rightarrow 0} \rho(\tau > \frac{\mu}{C}, \mathcal{B}) - \mu \exp^{-\mu\tau} < G(\mu(\mathcal{B})) \quad (1)$$

with C being a suitable normalizing factor and $G(\mu(\mathcal{B}))$ a function of the probability density measure, μ , in \mathcal{B} . The multifractal spectrum of return times has been investigated as well [10].

In this work, we extend this rigorous treatment to the case for which ϵ is far from zero and τ is arbitrary. This is motivated by the fact that experimentally only returns to regions of finite size can be observed. In the following we take the returning region to be a square of size ϵ intersecting the invariant set (attractor). We show that for both, nonhyperbolic (logistic map and Hénon map) and hyperbolic (Cat map) systems, the presence of recurrent trajectories that are not associated with UPOs inside the region increases as one increases the size of the region, causing the measure to become abnormally singular. In the case of nonhyperbolic systems, even for square of very small but finite size, the contribution to the measure of these recurrent trajectories is already large if the interval is close to a homoclinic tangency. Hence, as one observes a dynamical system for intervals of finite size, the local dynamics in \mathcal{B} can neither be completely governed by the linearization of these UPOs as proposed in the theorem of Hartman-Grobman [11], nor the measure inside the interval, $\mu(\mathcal{B})$, can be exactly calculated through the UPOs inside it. However, from the distribution of the FRTs we show that it is possible to calculate the measure exactly by introducing a correction of the measure from the eigenvalues of the UPOs inside the interval, when the intervals are far from small.

As already mentioned, an important result concerns the reconstruction of the measure using UPOs [5]. For hyperbolic systems, one can derive a formula to calculate the probability density, $\mu(\mathcal{B})_{EIG}$ of small squared subregions \mathcal{B} in the attractor. More explicitly

$$\mu(\mathcal{B})_{EIG} = \sum_{k=1}^{N_j} \left(\frac{1}{L_k} \right) \quad (2)$$

where the L_k are the positive eigenvalues of all fixed points located in \mathcal{B} of the j -fold iterate of the map, (i. e., the fixed points are period- j UPOs $\in \mathcal{B}$), and N_j represents the number of period- j UPOs $\in \mathcal{B}$.

We conveniently define a finite sized region to have a hyperbolic character if that region exhibits a distribution of FRTs close to a Poissonian. In this case, the measure, as well as the dynamics in that region, is described by the UPOs inside it, and typically there lie neither homo-

clinic tangencies nor low-period UPOs inside the region. Analogously, we define that a region is nonhyperbolic if the distribution of the FRTs deviates from a Poisson law. In that case, recurrent trajectories play an important role in the dynamics and in the contribution to the measure; here, typically low-period UPOs or homoclinic tangencies are found. We show that the larger the contribution of the recurrent trajectories to the measure is, the larger is the deviation of the calculation of the measure from the eigenvalues of the UPOs inside these intervals. The contribution becomes negligible as either the interval size tends to zero or the intervals are placed in hyperbolic regions and off homoclinic tangencies and low-period UPOs.

The probability measure in a square \mathcal{B} due to all the recurrent orbits (including the UPOs) with recurrent periods between τ_k and τ_l can be calculated from the distribution of the FRTs $\rho(\tau_i, \mathcal{B})$ as

$$\mu(\tau_k, \tau_l) = \frac{1}{\langle \tau(\mathcal{B}) \rangle} \sum_{i=k}^l \rho(\tau_i, \mathcal{B}), \quad (3)$$

where the average first return time is given by

$$\langle \tau(\mathcal{B}) \rangle = \lim_{n \rightarrow \infty} \frac{1}{n} \sum_{i=1}^n \tau_i(\mathcal{B}). \quad (4)$$

Note that if one sets in Eq. (3) $\tau_k = \tau_{min}$ (minimal FRT in \mathcal{B}) and $\tau_l = \tau_{max}$ (maximal FRT in \mathcal{B}), then, $\sum_{i=\tau_{min}}^{\tau_{max}} \rho(\tau_i, \mathcal{B}) = 1$ and one recovers Kac's theorem, which states that

$$\mu(\mathcal{B}) = \frac{1}{\langle \tau(\mathcal{B}) \rangle}, \quad (5)$$

with $\langle \tau(\mathcal{B}) \rangle$ the average FRT, relating a time averaged quantity $\langle \tau(\mathcal{B}) \rangle$ with a spatial quantity, $\mu(\mathcal{B})$.

In order to calculate the measure exclusively due to UPOs inside \mathcal{B} , we hypothesize that the distribution of the FRTs can be split into two discrete functions (for a small FRTs) and into two continuous functions (for large FRTs), one describing the contribution due to the UPOs and the other the contribution of the recurrent trajectories, respectively. Hence,

$$\mu'(\mathcal{B}) = \mu(\mathcal{B})_{REC}^d + \mu(\mathcal{B})_{UPO}^d + \mu(\mathcal{B})_{REC}^c + \mu(\mathcal{B})_{UPO}^c, \quad (6)$$

with $\mu(\mathcal{B})_{REC}^d = \frac{1}{\langle \tau(\mathcal{B}) \rangle} \sum_{i=\tau_{REC}} \rho(\tau_i, \mathcal{B})$, $\mu(\mathcal{B})_{UPO}^d = \frac{1}{\langle \tau(\mathcal{B}) \rangle} \sum_{i=\tau_{UPO}} \rho(\tau_i, \mathcal{B})$, and

$$\mu(\mathcal{B})_{REC}^c = \frac{1}{\langle \tau(\mathcal{B}) \rangle} \int_{\tau_{UPO}^{min}}^{\tau_{max}} \beta_{REC} \exp(-\alpha\tau) d\tau \quad (7)$$

$$\mu(\mathcal{B})_{UPO}^c = \frac{1}{\langle \tau(\mathcal{B}) \rangle} \int_{\tau_{UPO}^{min}}^{\tau_{max}} \alpha \exp(-\alpha\tau) d\tau. \quad (8)$$

The index d designates a discrete summation and c indicates a continuous integral. $\mu(\mathcal{B})_{REC}^d$ is the measure

due to short recurrent trajectories, $\mu(\mathcal{B})_{UPO}^d$ due to low-period UPOs, $\mu(\mathcal{B})_{REC}^c$ the measure due to long recurrent trajectories and $\mu(\mathcal{B})_{UPO}^c$ due to high-period UPOs [14]. The return time τ_{REC} stands for first returns that are different from any of the period of the UPOs inside \mathcal{B} , and τ_{UPO} for all periods of the UPOs. The time τ_{UPO}^{min} corresponds to the minimum period for which one can consider the distribution of FRT to be well described by a continuous exponential function and the measure can be calculated with the Eqs. (7) and (8). These two integrals are constructed under the assumption that the probability distribution is given by

$$\rho(\tau, \mathcal{B}) = \beta \exp^{-\alpha\tau}, \quad (9)$$

i.e., it agrees with Eq. (1). Since $\mu(\mathcal{B}) \propto \epsilon^{D_p}$, $D_p > 0$ being the pointwise dimension for that interval [13], as $\epsilon \rightarrow 0$ and $\tau > \frac{\mu}{C}$, the distribution (9) should approach a Poisson function $\rho(\tau, \mathcal{B}) = \mu \exp^{-\mu\tau}$. Equation (9) can be broken in a summation of two distributions, one due to the long recurrent trajectories $\rho_{REC}^c = \beta_{REC} \exp(-\alpha\tau)$, and the other due to the large-period UPOs, a Poissonian of the type $\rho_{UPO}^c = \alpha \exp(-\alpha\tau)$, such that $\rho_{REC}^c + \rho_{UPO}^c = \beta \exp(-\alpha\tau)$. Therefore, $\beta_{REC} + \alpha = \beta$, and, from Eq. (1), as $\epsilon \rightarrow 0$, $\beta_{REC} = 0$, and $\alpha = \mu$. The coefficients β and α are obtained by fitting the distribution of the FRTs by an exponential of the form of Eq. (9). Integrating Eqs. (7) and (8) we get $\mu_{REC}^c = \left(\frac{\beta}{\alpha} - 1\right) \gamma \mu$ and $\mu_{UPO}^c = \gamma \mu$, with $\gamma = \exp^{-(\tau_{UPO}^{min})\alpha} - \exp^{-(\tau_{max})\alpha}$.

Assuming that μ_{REC}^d and μ_{UPO}^d are negligible in comparison with μ_{REC}^c and μ_{UPO}^c , and that $\mu_{EIG} = \mu_{UPO}^c$ (what is true for moderately nonhyperbolic regions which are predominant in the attractor), we arrive at a formula that expresses the value of the measure through the measure calculated exclusively with the contribution from the UPOs inside \mathcal{B}

$$\mu(\mathcal{B}) \cong K \mu(\mathcal{B})_{EIG}, \quad (10)$$

where $\frac{1}{K} = \left(1 - \gamma \left[\frac{\beta}{\alpha} - 1\right]\right)$.

Our model of a nonhyperbolic system is the Hénon map, $H : \mathcal{X} \rightarrow \mathcal{X}$, $x_{i+1} = a - x_i^2 + b y_i$, and $y_{i+1} = x_i$, with $a = 1.4$ and $b = 0.3$. The nonhyperbolicity of this map is due to tangencies of the stable and unstable manifolds of periodic orbits embedded in the chaotic attractor.

In Fig. 1 we show what should be expected from a hyperbolic and from a nonhyperbolic region. In Fig. 1(a), points represent all the UPOs up to period 23, calculated using the method of Ref. [4], and stars depict the primary tangencies together with their five images and preimages, where primary indicates that the curvature of the manifold is minimal in their neighborhood. In Fig. 1(b) we display a typical nonhyperbolic region (box) centered at the primary tangency $T_1 : (x, y) = (1.7801, -0.0949)$ with box size $\epsilon = 0.02$. The lowest periodic orbit found in that region has period 18, whereas the smallest FRT is $\tau = 9$. Points represent

the Hénon attractor, and the filled circle a component of a period-9 orbit. The stripe marked by W_s pictures points inside \mathcal{B} that under H^9 (the 9-fold iterate of the map H) remain in the interval, represented by W_u . As one can see, the stripes W_s and W_u are aligned along the stable and unstable manifold of the period-9 orbit located outside \mathcal{B} . Consequently, the tangency creates recurrent trajectories that are not associated with any UPO inside \mathcal{B} . Note that, as could be anticipated for a nonhyperbolic region, the stripes W_s and W_u are almost parallel close to T_1 . In Fig. 1(c) we demonstrate that a similar effect occurs when there is a low-period UPO inside \mathcal{B} (here of period-2). Although there exists no period-13 UPO, we nevertheless find a FRT of $\tau=13$. That is caused by points on the stripes W_s and W_u , which lie on the stable and unstable manifold of a period-13 orbit outside \mathcal{B} . Finally, we show in Fig. 1(d) a typical hyperbolic region, where to all observed FRTs of length τ a period- τ UPO inside \mathcal{B} corresponds, and the manifolds cross transversally.

FIG. 1: Points represent the chaotic attractor Γ , filled circles periodic orbits, and W_s denotes points inside \mathcal{B} that under H^P (where P is the period of the UPO) remain in the interval; their P -fold iteration is shown by W_u . In (b) the box is centered in a primary tangency and in (c) in a low-period UPO. Both are typical nonhyperbolic regions. In (d) a characteristic hyperbolic region is depicted.

To quantify now these findings with our theory, we analyze two specific intervals with $\epsilon = 0.02$, a nonhyperbolic one, \mathcal{B}_1 , centered at the primary tangency T_1 , see Fig. 1(b), and a hyperbolic one, \mathcal{B}_2 , centered at the point $(x, y) = (1.1181, 0.1472)$, see Fig. 1(d), for which the smallest period of all UPOs is found to be 21, and no tangency is present.

For the nonhyperbolic interval \mathcal{B}_1 , we get $\mu_{REC}^d = 1.28 \times 10^{-4}$ from the return times $\tau_{REC} = (9, 16, 17, 18, 19, 20, 22)$, $\mu_{UPO}^d = 0$, $\mu_{REC}^c = 2.41 \times 10^{-5}$, and $\mu_{UPO}^c = 2.885 \times 10^{-3}$, with $\tau_{UPO}^{min} = 23$ and $\tau_{max} = 4284$ in Eqs. (7), (8), obtained by measuring 400,000 returns to that interval. Employing Eq. (6), this yields a measure of $\mu' = 3.0923 \times 10^{-3}$. We stress that the measure evaluated using Kac's lemma with 400,000 returns, considered to be the exact one, leads to $\mu = 3.100 \times 10^{-3}$, very close to our estimate from Eq. (6). We see further that most of the measure is due to the UPOs and the contribution from recurrent trajectories μ_{REC}^d and μ_{REC}^c can be neglected. From Eq. (2) the best estimate (determined for UPOs of up to period 30) is $\mu_{EIG} = 3.003 \times 10^{-3}$. Note that $\mu_{EIG} \cong \mu_{BOTH}^d + \mu_{UPO}^c$. In spite of this region being strongly nonhyperbolic, we apply nevertheless the correction in Eq. (10), which yields $\mu(\mathcal{B}) = 3.027 \times 10^{-3}$, a value closer to the exact μ than μ_{EIG} .

The hyperbolic region \mathcal{B}_2 results in $\mu_{REC}^d = 0$, $\mu_{UPO}^d = 0$, $\mu_{REC}^c = 9.97 \times 10^{-6}$, and $\mu_{UPO}^c = 7.712 \times 10^{-4}$, with $\tau_{UPO}^{min} = 23$ and $\tau_{max} = 16871$ obtained for 400,000

returns to that interval as before. This gives with Eq. (6) $\mu' = 7.2295 \times 10^{-4}$, whereas the exact measure, using Eq. (5), ensues $\mu = 7.2422 \times 10^{-4}$, very close to the value obtained with the correction formula Eq. (6). Again, most of the measure is due to the UPOs. From Eq. (2) the best estimate (calculated for UPOs of up to period 30) of $\mu_{EIG} = 7.5312 \times 10^{-4}$. For this case, Eq. (10) has no use since $\mu_{EIG} > \mu$.

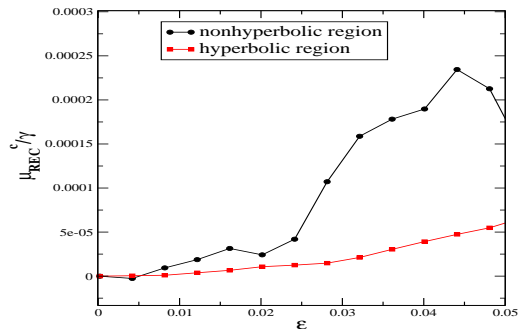


FIG. 2: The weighted measure $\frac{\mu(\mathcal{B}_i)^c_{REC}}{\gamma}$, $i=1, 2$, due to recurrent trajectories with respect to ϵ for the interval \mathcal{B}_1 (circles) and \mathcal{B}_2 (squares).

To understand how the recurrent trajectories contribute to the measure of these two intervals when the boxsize ϵ varies, in Fig. 2 the value of $\frac{\mu(\mathcal{B}_i)^c_{REC}}{\gamma} = (\frac{\beta}{\alpha} - 1)\mu(\mathcal{B}_i)$, $i = 1, 2$ is plotted against ϵ . It can be calculated using only the information of the FRTs, and thus there is no need of knowing τ_{UPO}^{min} , a numerically involving task. We see that for the interval \mathcal{B}_1 , centered at the primary tangency T_1 , the contribution of the recurrent trajectories $\mu_{REC}(\mathcal{B}_1)$ is much larger than $\mu_{REC}(\mathcal{B}_2)$ for the interval \mathcal{B}_2 , provided $\epsilon > 0.0002$. It grows moreover much faster with increasing ϵ . Also, for \mathcal{B}_2 this contribution decays smoothly as one decreases ϵ . This smooth decay in arbitrary intervals of finite size takes typically place in hyperbolic regions when the size approaches zero. It is also encountered in the hyperbolic cat map as well as in the hyperbolic regions of the logistic map [9].

In Fig. 3 we plot $|\langle \frac{\mu(\mathcal{B}_i)^c_{REC}}{\gamma \mu(\mathcal{B}_i)} \rangle|$ (squares), $|\langle \frac{\mu(\mathcal{B}_i) - \mu(\mathcal{B}_i)_{EIG}}{\mu(\mathcal{B}_i)} \rangle|$ (circles), and $|\langle \frac{\mu(\mathcal{B}_i) - K \mu(\mathcal{B}_i)_{EIG}}{\mu(\mathcal{B}_i)} \rangle|$ (diamonds) versus ϵ , in a log-log graph. The average is performed over intervals \mathcal{B}_i centered in consecutive points of a trajectory of length 5000 and $\mu(\mathcal{B}_i)_{EIG}$ is calculated using the set of all UPOs of period 29. The standard deviation bar is also shown in this figure. Whenever $\frac{\beta}{\alpha} < 0$, which indicates the presence of low-period UPO inside the interval, $\mu(\mathcal{B}_i)_{UPO}^d$ cannot be neglected, and therefore the approximation proposed in Eq. (10) cannot be used. Furthermore, the calculation of the measure from Eq. (2) oscillates widely in intervals dominated by low-period UPOs, since one considers different sets of UPOs with varying periods.

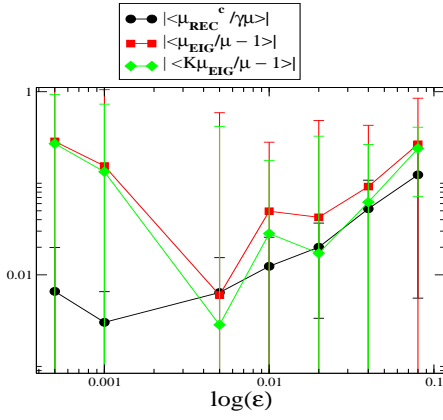


FIG. 3: Averages $|\langle \frac{\mu(\mathcal{B}_i)^c}{\gamma \mu(\mathcal{B}_i)} \rangle|$ (squares), $|\langle \frac{\mu(\mathcal{B}_i) - \mu(\mathcal{B}_i)^{EIG}}{\mu(\mathcal{B}_i)} \rangle|$ (circles), and $|\langle \frac{\mu(\mathcal{B}_i) - K \mu(\mathcal{B}_i)^{EIG}}{\mu(\mathcal{B}_i)} \rangle|$ (diamonds), $i = 1, 2, \dots, 5000$, against ϵ , in a log-log graph.

Consequently, the averages calculated in this figure are restricted to intervals with $\frac{\beta}{\alpha} > 0$. Additionally, τ_{UPO}^{min} is considered to be approximately given by τ_{REC}^{min} . As a result, in an average sense, the presence of recurrent

trajectories (circles) significantly affects the correctness of the calculation of the measure from the eigenvalues of the UPOs in Eq. (2) (squares). It is apparent from the figure that, on average, the correction proposed in Eq. (10) for μ_{EIG} yields a value closer to the real measure μ , as well as a lower standard deviation.

In conclusion, finite size regions of chaotic attractors can generally be classified in two categories, hyperbolic and nonhyperbolic ones. For the former, the measure is almost completely supported by the UPOs inside the region and the distribution of the returns close to a Poissonian, while for the latter, the contribution of the recurrent trajectories not associated to UPOs inside the region is significant and the return time distribution deviates from a Poissonian. In this case an exact calculation of the measure can only be performed from the first return times. This has strong implications on experiments, as there only finite region can be monitored and many systems are nonhyperbolic.

M. S. B. and S. K. acknowledge support by the Alexander von Humboldt foundation, a stay at IMPA, and discussions with V. Sidoravicius and O. de Almeida. C. G. and partially also M. S. B. were financed by FAPESP.

-
- [1] J.-P. Eckmann and D. Ruelle, Rev. Mod. Phys. **57**, 617 (1985).
 - [2] D. Auerbach, *et al.*, Phys. Rev. Lett. **58**, 2387 (1987).
 - [3] M. H. Jensen, L. P. Kadanoff, and I. Procaccia, Phys. Rev. A **36**, 1409 (1987); G. H. Gunaratne and I. Procaccia, Phys. Rev. Lett. **59**, 1377 (1987); P. Cvitanović, Phys. Rev. Lett. **61**, 2729 (1988).
 - [4] O. Biham and W. Wenzel, Phys. Rev. Lett. **63**, 819 (1989).
 - [5] C. Grebogi, E. Ott, and J. A. Yorke, Phys. Rev. A **36**, 3522 (1987); Phys. Rev. A **37**, 1711 (1988).
 - [6] Y.-C. Lai, Y. Nagai, and C. Grebogi, Phys. Rev. Lett. **79**, 649 (1997).
 - [7] M. Hirata, B. Saussol, and S. Vaienti, Comm. Math. Phys. **206**, 33 (1999).
 - [8] G. M. Zaslavsky and M. K. Tippet, Phys. Rev. Lett. **67**, 3251 (1991); V. Afraimovich and G. M. Zaslavsky Phys. Rev. E **55**, 5418 (1997).
 - [9] M. S. Baptista, *et al.*, Physica (Amsterdam) **287A**, 91 (2000); M. S. Baptista, *et al.*, Phys. Plasmas **8**, 4455 (2001).
 - [10] N. Hadyn, *et al.*, Phys. Rev. Lett. **88**, 224502 (2002).
 - [11] P. Hartman, Proc. Amer. Math. Soc. **11**, 610 (1960); D. M. Grobman, Dokl. Akad. Nauk SSSR **128**, 880 (1960).
 - [12] M. Kac, Bull. Am. Math. Soc. **53**, 1002 (1947).
 - [13] J. D. Farmer, E. Ott, and J. A. Yorke, Physica (Amsterdam) **7D**, 153 (1983).
 - [14] In the examples that follow, the border of short and long orbits is of a period of about 20. However, the exact value is not of crucial importance.